





Article

Production of Human Milk Fat Substitutes by Lipase-Catalyzed Acidolysis: Immobilization, Synthesis, Molecular Docking and Optimization Studies

Cleide M. F. Soares^{1,2}, Milson S. Barbosa³, Samuel B. Santos¹ , Silvana Mattedi⁴, Álvaro S. Lima^{1,2},
Matheus M. Pereira⁵ , Carla Tecelão⁶  and Suzana Ferreira-Dias^{7,*} 

- ¹ Programa de Pós-Graduação em Engenharia de Processos, UNIT—Universidade Tiradentes, Av. Murilo Dantas, 300, Farolândia, Aracaju 49032-490, SE, Brazil; cleide.mara@souunit.com.br (C.M.F.S.); samuelbruno@gmail.com (S.B.S.); aslima2001@yahoo.com.br (Á.S.L.)
 - ² ITP—Instituto de Tecnologia e Pesquisa, Av. Murilo Dantas, 300, Prédio do ITP, Farolândia, Aracaju 49032-490, SE, Brazil
 - ³ IFPB—Instituto Federal de Educação, Ciência e Tecnologia da Paraíba, Campus Cajazeiras, Rua José Leônicio da Silva, 300, Jardim Oasis, Cajazeiras 58900-000, PB, Brazil; milson.barbosa@ifpb.edu.br
 - ⁴ UFBA—Departamento de Engenharia Química, Universidade Federal da Bahia, Rua Aristides Novis 2, Federação, Salvador 40210-630, BA, Brazil; silvana@ufba.br
 - ⁵ CIEPQPF—Department of Chemical Engineering, University of Coimbra, Rua Sílvio Lima, Pólo II—Pinhal de Marrocos, 3030-790 Coimbra, Portugal; matheus@eq.uc.pt
 - ⁶ MARE—Marine and Environmental Sciences Centre, ARNET—Aquatic Research Network, ESTM, Politécnico de Leiria, 2520-630 Peniche, Portugal; carla.tecelao@ipleiria.pt
 - ⁷ LEAF—Linking Landscape, Environment, Agriculture and Food, Associated Laboratory TERRA, Laboratório de Estudos Técnicos, Instituto Superior de Agronomia, Universidade de Lisboa, Tapada da Ajuda, 1349-017 Lisbon, Portugal
- * Correspondence: suzanafdias@mail.telepac.pt



Citation: Soares, C.M.F.; Barbosa, M.S.; Santos, S.B.; Mattedi, S.; Lima, Á.S.; Pereira, M.M.; Tecelão, C.; Ferreira-Dias, S. Production of Human Milk Fat Substitutes by Lipase-Catalyzed Acidolysis: Immobilization, Synthesis, Molecular Docking and Optimization Studies. *Catalysts* **2023**, *13*, 825. <https://doi.org/10.3390/catal13050825>

Academic Editor: Chiching Hwang

Received: 30 March 2023

Revised: 23 April 2023

Accepted: 25 April 2023

Published: 29 April 2023



Copyright: © 2023 by the authors. Licensee MDPI, Basel, Switzerland. This article is an open access article distributed under the terms and conditions of the Creative Commons Attribution (CC BY) license (<https://creativecommons.org/licenses/by/4.0/>).

Abstract: Human milk fat (HMF) triacylglycerols (TAGs) mainly contain palmitic acid esterified at the *sn*-2 position while oleic and other unsaturated fatty acids are located at positions *sn*-1,3. This study aimed at the production of HMF substitutes (HMFS) by lipase-catalyzed acidolysis of tripalmitin with oleic acid, in a solvent-free medium. *Burkholderia cepacia* lipase (BCL) was immobilized in silica (prepared with protic or aprotic ionic liquids) by covalent binding or encapsulation and used as biocatalyst. The supports and immobilized biocatalysts were characterized by FTIR, TGA, and SEM. Molecular docking analysis showed that BCL preferentially attacks oleic acid rather than tripalmitin, due to the lower free energy of hydrophobic binding with this acid ($-6.5 \text{ kcal}\cdot\text{mol}^{-1}$) than with tripalmitin ($5.4 \text{ kcal}\cdot\text{mol}^{-1}$). Therefore, the tripalmitin attack by BCL and subsequent HMFS production only occurs after the binding to most of the oleic acid molecules. The highest acidolysis activity was obtained with BCL immobilized by covalent binding in prepared silica with aprotic ionic liquid. A central composite rotatable design, as a function of temperature ($58\text{--}72 \text{ }^\circ\text{C}$) and oleic acid/tripalmitin molar ratio ($\text{MR} = 2:1\text{--}6.8:1$), was performed for acidolysis optimization. Under optimized conditions ($58 \text{ }^\circ\text{C}$ and $\text{MR} = 4:1$ or $60 \text{ }^\circ\text{C}$ and $\text{MR} = 2:1$), the oleic acid incorporation of 28 mol.% was achieved after 48 h.

Keywords: human milk fat substitutes; immobilization; ionic liquid; lipase; molecular docking

1. Introduction

Structured lipids, i.e., novel lipids with functional properties that do not exist in nature, have been obtained by lipase-catalyzed reactions [1–3]. Among structured lipids, the synthesis of human milk fat substitutes (HMFS) that mimic human milk fat (HMF) has been a challenge for the food industry. This is a hot topic, as demonstrated by the recent reviews on enzymatic synthesis of HMFS [4–9]. In human milk fat, palmitic and oleic acids (P and O) are the two most abundant fatty acids (FA). Palmitic acid represents about a quarter of the

total milk FA and is located primarily at the *sn*-2 position (>60 mol.%), whereas the *sn*-1,3 positions are mainly occupied by oleic acid. Thus, the major triacylglycerol (TAG) of human milk is *sn*-1,3-dioleoyl-2-palmitoylglycerol (OPO). The presence of palmitic acid at the *sn*-2 position is of great importance for the absorption of fat and minerals in infants [7,10]. Therefore, OPO is the target TAG used as a supplement in infant formulas [11].

HMFS are usually obtained by enzyme-catalyzed (i) acidolysis of TAGs with free fatty acids, or (ii) by interesterification of TAGs with fatty acid ethyl esters. These reactions can be performed either in the presence or in the absence of an organic solvent, catalyzed by commercial or non-commercial *sn*-1,3 immobilized lipases. Different substrates, such as tripalmitin, lard, butterfat, or palm stearin, as the source of TAGs having palmitic acid at position *sn*-2, and different operation conditions, have been used. Free fatty acids (FFA), namely oleic acid or polyunsaturated fatty acids (linoleic, linolenic, arachidonic, or docosahexaenoic (DHA) acids), essential for infant growth and development, or their ethyl esters, have been used as acyl-donors [12–16]. The presence of approximately 0.3% DHA in infant formula has recognized beneficial effects in infants during their first year, as reported by the European Food Safety Authority [7].

Currently, there are several products in the market, obtained by enzymatic processes, that are used as HMFS in infant formulas. Their formulation varies with the country. For example, lard is used as source of palmitic acid at the *sn*-2 position in HMFS produced in Japan. However, due to religious, labeling, and safety issues, this fat is not used in several countries [7].

Betapol was the first OPO product developed in 1986 by Bunge Loders Croklaan [17]. It was launched in the market as HMFS, after European approval in 1995. Betapol is obtained by acidolysis catalyzed by immobilized *sn*-1,3 regioselective *R. miehei* lipase [11]. Currently, there is a portfolio of Betapol products, including “Betapol Plus Blend 60” containing 60% of *sn*-2 palmitate. Moreover, Betapol is the first certified OPO according to both EU Organic and China Organic Standards [17].

INFAT is a similar product with OPO as the main TAG, from Advanced Lipids [18]. Some formulations contain 52% (e.g., INFAT; INFAT PLUS, INFAT ORGANIC) or more than 60% (INFAT PRO) of *sn*-2 palmitate [18]. More recently, Wilmar International launched in the market MILKOPAS, which is an OPO product to be used as HMFS [19].

In biocatalysis, it is recommended to use lipases in an immobilized form to reduce the cost and retain or even increase the stability of free lipases [20]. However, the search for novel immobilized lipases presenting high activity and operational stability is mandatory to make enzymatic processes competitive, mainly in the production of commodity fats.

Recently, in the immobilization process, the ionic liquids (ILs) have been used as additives to increase the enzyme activity and stability [21–23]. ILs are important additives for immobilization, due to the ease of synthesis, nonflammability, and high chemical and thermal stabilities, favoring industrial applications [24–28]. The *Burkholderia cepacia* lipase (BCL) was successfully immobilized in the presence of ILs by our group [21,29]. This biocatalyst showed 35-fold total activity in hydrolysis reaction, compared with the activity of the immobilized enzyme without any additive [29]. Despite the excellent results obtained in terms of enzymatic activity, the use of protic or aprotic ILs for support preparation and BCL immobilization by covalent binding and encapsulation, for subsequent application in production of HMFS, has not been attempted yet.

In process optimization, the classical approach of testing one variable at a time (OVAT) needs a large number of experiments and, in most of the cases, an apparent optimum is reached since the interactions between variables are not considered. The use of adequate experimental designs, where several variables (factors) are handled simultaneously, such as those used in response surface methodology (RSM), have several advantages over the OVAT procedure. Using RSM designs allows for (i) the detection of eventual interactions between factors, (ii) an easy and efficient way to estimate the main effects of the factors, and (iii) the substantial reduction in the number of experiments (and costs) having the same precision as the classical approach. Moreover, a response surface described by a polynomial

model, as a function of the independent factors, can be fitted to the experimental data-points. From the response surface model, it is possible to model the process and find the best conditions to attain the optimal response [30].

Several studies showed the relevant application of RSM for modelling and optimization of the production of human milk fat substitutes by lipase-catalyzed acidolysis [14,15,31].

Therefore, the aim of the present study was to test BCL immobilized in hydrophobic modified silica matrices, using the sol-gel technique, in presence of protic or aprotic ionic liquids, by two immobilization methods (covalent binding and encapsulation), as catalyst for the production of HMFS by acidolysis of tripalmitin with oleic acid, in a solvent-free medium. Molecular docking analysis was performed for BCL against tripalmitin and oleic acid molecules to elucidate the time-course of acidolysis reaction. Furthermore, the production of HMFS was optimized considering the combination of temperature and the molar ratio (oleic acid: tripalmitin) effects, using RSM.

2. Results and Discussion

2.1. Selection of Immobilization Strategies

In this work, the BCL was immobilized by covalent binding (C) or encapsulation (E) in silica without the presence of IL, and silica prepared in the presence of protic (PIL) or aprotic (AIL) IL. Figure 1 shows the incorporation values (mol.%) of oleic acid in tripalmitin for the different immobilized biocatalysts, obtained by acidolysis at 60 °C, using a molar ratio oleic acid/tripalmitin of 2:1 and a load of 5% biocatalyst (*w/w*). The schematic of the lipase-catalyzed reaction of acidolysis of tripalmitin with oleic acid is presented by Ferreira-Dias et al., 2022 [3].

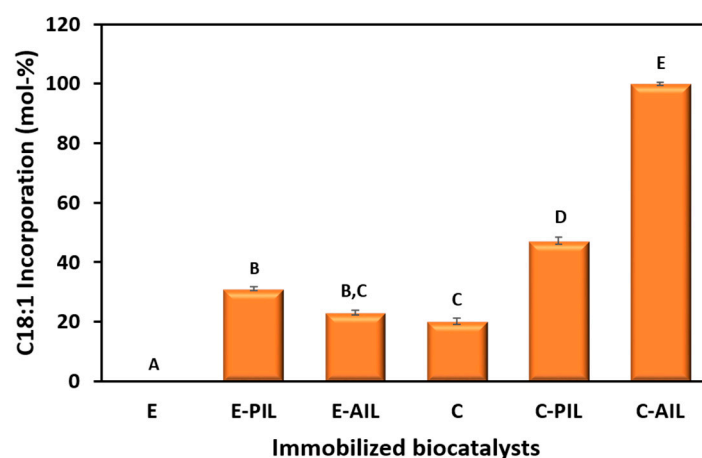


Figure 1. Incorporation (mol.%) of oleic acid in tripalmitin, after 48 h of acidolysis reaction catalyzed by BCL immobilized by covalent binding (C) or encapsulation (E) on silica prepared in absence or in presence of protic (PIL) or aprotic (AIL) ILs. Acidolysis was carried out at 60 °C, molar ratio oleic acid/tripalmitin of 2:1, and 5% biocatalyst (*w/w*). Bars represent the standard errors. For each response, bars with different letters indicate differences based on the Tukey test ($p \leq 0.05$).

Overall, the use of these ILs as modifying agents in the synthesis of silica leads to a positive effect on the efficiency of immobilized BCL favoring the incorporation of oleic acid in tripalmitin (values of incorporation ranging between 4.7 and 23.5 mol.%) when compared to the BCL immobilized on silica prepared with no ILs present (0 by encapsulation and 5 mol.% by covalent binding). Concerning the production of HMFS by enzymatic acidolysis, the best results (oleic acid incorporation in TAGs) were obtained using the lipase covalently bound on the modified silica previously silanized and activated with glutaraldehyde in the presence of the AIL (C-AIL, 23.5 mol.% oleic acid incorporation), followed by the results obtained with the lipase covalently bound in the presence of the

protic ionic liquid (C-PIL, 11.1 mol.% incorporation). When the lipase was immobilized by encapsulation in the absence of IL, no acidolysis activity was observed.

Thus, the best results of relative incorporation were obtained using the lipase covalently bound on silica prepared with AIL (C-AIL, 23.5 mol.% oleic acid incorporation), followed by the results obtained with the lipase covalently bound in the presence of the protic ionic liquid (C-PIL, 11.1 mol.% incorporation). The lower performance of BCL immobilized by encapsulation (E-AIL and E-PIL) in acidolysis may be explained by diffusion transfer limitations of free fatty acids within the sol-gel matrix [29]. When the lipase was immobilized by encapsulation in the absence of IL, no acidolysis activity was observed. Therefore, the catalytic efficiency of the immobilized biocatalyst depends upon its morphological and physicochemical characteristics since its properties have an impact on the substrate diffusion process.

2.2. Physicochemical and Morphological Characterization of the Immobilized Biocatalysts

To understand the different behaviors exhibited by the immobilized biocatalysts, analysis for physicochemical (FTIR and TGA), and morphological (SEM) characterization were performed.

The efficiency of BCL immobilization by covalent binding and encapsulation through the presence of protein was evaluated by FTIR. Figure 2 shows the FTIR spectra of the support, free BCL, and immobilized biocatalysts (E-PIL, E-AIL, C-PIL, and C-AIL). The peaks at 696 cm^{-1} can be related to both amide IV and V (bands characteristics of proteins) showing the presence of BCL in the immobilized systems (C-PIL, E-PIL, C-AIL, and E-AIL). Amides IV and V are respectively due to OCN bending and out-of-plane NH bending, as described by Carvalho et al., 2018 [32]. Spectra were performed in the amide I region ($1700\text{--}1600\text{ cm}^{-1}$) because this region is light on conformational changes for free BCL.

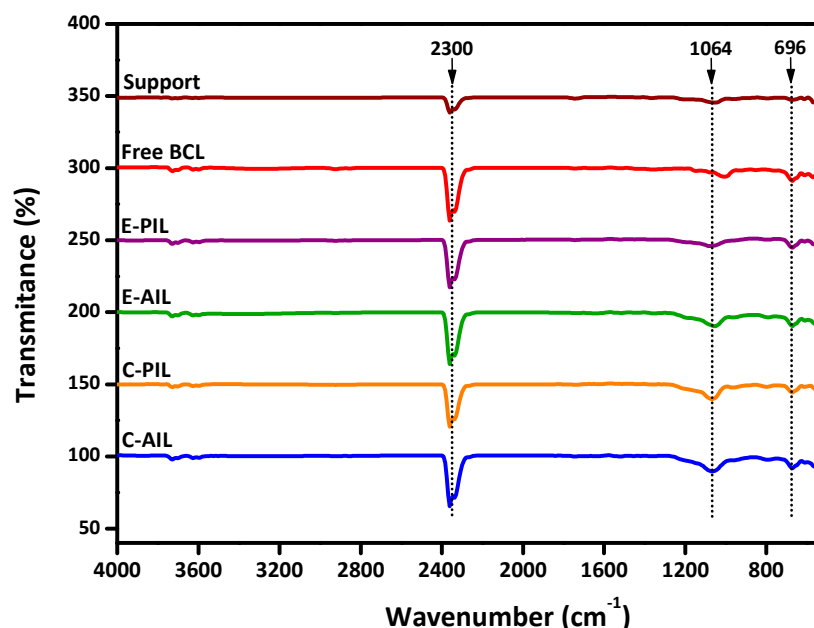


Figure 2. FTIR spectra of the support, free BCL, and immobilized biocatalysts (E-PIL, E-AIL, C-PIL, and C-AIL).

This confirms that the enzyme molecules are retained after immobilization in the support materials [33,34]. For the support, free of enzyme, no peaks in this region were observed, which is explained by the absence of enzyme molecules. The presence of bands characteristic of silica, such as Si–O–Si asymmetric stretching groups, are noticed at 1064 cm^{-1} . The percentage of transmittance at higher wavenumber peaks (2200 and 2400 cm^{-1}) greatly decreased in the immobilized lipases, followed by free enzyme, and to a lesser extent for the support. Additionally, the spectrum for C-AIL shows an intense band at 2300 cm^{-1}

probably due to asymmetric stretching of the Si–O–Si chain of the support and contributions of amide III. This can be related to the highest acidolysis activity observed with this immobilized preparation. The lowest transmittance of the peaks at 2300 cm^{-1} resulting from the characteristics of silica structure, was observed for BCL immobilized by encapsulation on the prepared silica in the presence of the protic ionic liquid (E-PIL). This IL may modify the stereometric characteristics of immobilized lipase. In addition, water immiscible ILs, such as [bmim][PF₆], form a strong ionic matrix which retains lipase molecules in an adequate microenvironment, consisting of a supramolecular net that will be able to keep the active protein conformation [35].

In addition to FTIR analysis, the mass losses of samples of support, free BCL, and immobilized biocatalysts were determined by thermogravimetric analysis (TGA). Figure 3 shows the TGA curves for all the characterized BCL immobilized by covalent binding in silica prepared in the presence of IL aprotic (C-AIL). The TGA graphs can be divided into 3 main parts: the region of solvent evaporation (room temperature up to $220\text{ }^{\circ}\text{C}$), the region of the crosslinking process ($220\text{--}320\text{ }^{\circ}\text{C}$), and the region of degradation ($320\text{--}650\text{ }^{\circ}\text{C}$). As shown in Figure 3, the highest mass loss was observed for the free enzyme (80% loss), while only 22.1% weight loss was observed for the support sample. This weight loss can be attributed to the presence of unreacted silanol groups from the TEOS, which are present in the silica because of incomplete sol-gel reaction [36]. Additionally, the removal of water molecules, tightly bound to the silica matrix, might occur [37]. The matrices with immobilized lipase by covalent binding showed similar values of mass loss (24.6% for C-AIL and 26.80% for C-PIL). However, in the samples with immobilized enzyme by encapsulation, higher mass losses were observed (32.2% for E-AIL and 33.0% for E-PIL). Soares et al., 2004 [38] correlated a lower mass loss of immobilized lipase with interactions between silane precursors and organic components (additives and lipase). This may be ascribed to the presence of water molecules associated to the cations or anions. This water may be either fixed to the support or in free form, occupying positions in the lattice of the sol-gel matrix in the presence of the AIL [29].

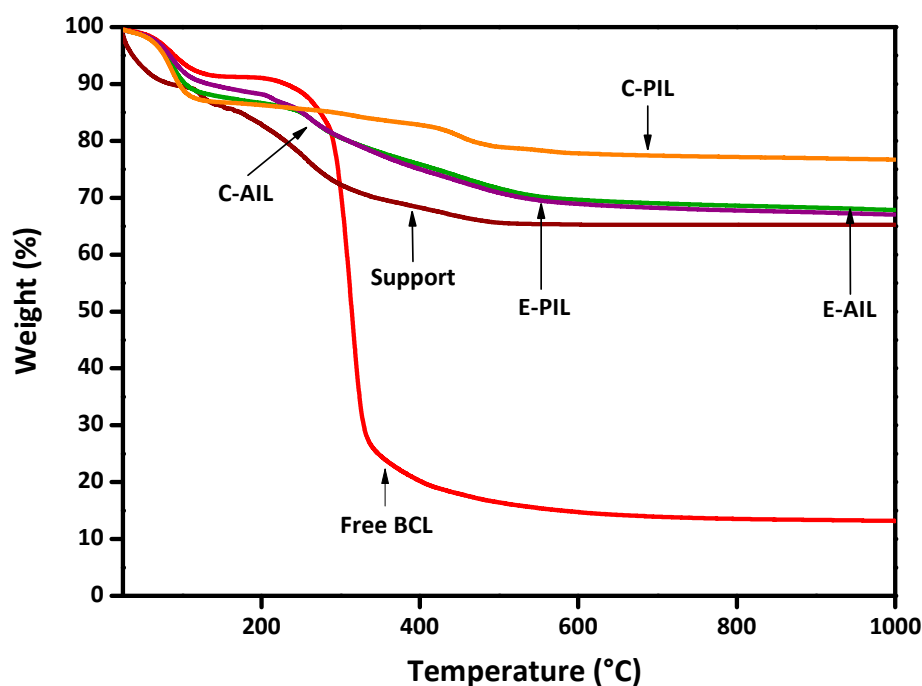


Figure 3. Thermogravimetric curves at $20\text{ }^{\circ}\text{C min}^{-1}$ under nitrogen atmosphere of the support, free BCL, and immobilized biocatalysts (E-PIL, E-AIL, C-PIL, and C-AIL).

Differences in the surface morphology of the support and of the most efficient immobilized biocatalyst for acidolysis (C-AIL) were investigated by SEM. Figure 4 shows

the micrographs of the support (Figure 4a) and the BCL immobilized by covalent binding in silica prepared in the presence of IL aprotic (C-AIL) (Figure 4b). In Figure 4a, a rigid superficial structure, probably forming only one block, can be observed. In the immobilized preparation obtained by covalent binding (C-AIL), the surface appears to be occupied with lipase molecules that are covalently bonded to the silica surface, explaining the higher acidolysis efficiency of this biocatalyst. These micrographs demonstrate that the use of IL aprotic during silica preparation promotes a more irregular and fissured surface and, consequently, the efficiency of BCL immobilization [39].

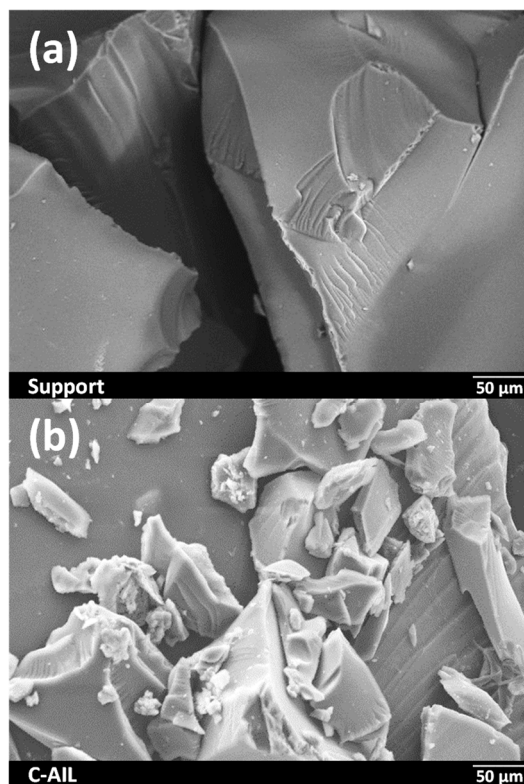


Figure 4. Scanning electron micrographs of: (a) support, and (b) immobilized BCL by covalent binding on support prepared in presence IL aprotic (C-AIL).

2.3. Time-Course of Acidolysis and Molecular Docking Study

The time-course of acidolysis catalyzed by immobilized BCL on support prepared in the presence of IL aprotic (C-AIL) in a solvent-free medium was performed under the same conditions followed in the biocatalyst screening experiments. The results, as illustrated in Figure 5, demonstrated that the incorporation rate of oleic acid in tripalmitin was very low during the first 10 h reaction time. Moreover, the degree of the incorporation increased with the increasing reaction time, and quasi-equilibrium was attained only after 48 h, with oleic acid incorporation of about 27.6 mol.%. It is worth mentioning that the incorporation of oleic acid only occurs after catalysis of the *sn*-1,3-position of the triacylglycerol backbone, which in this case is tripalmitin. This result is very close to the theoretical maximum incorporation of 31.5 mol.%, expected when the stoichiometric value acyl donor/tripalmitin (MR = 2:1) is used [16].

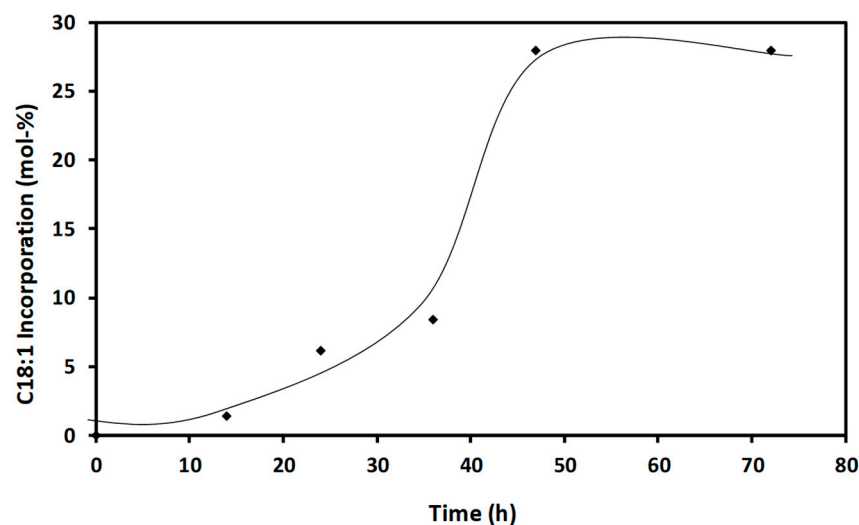


Figure 5. Time-course of acidolysis of tripalmitin with oleic acid catalyzed by immobilized BCL by covalent binding on support prepared in the presence of aprotic IL (C-AIL), at 60 °C, molar ratio oleic acid/tripalmitin of 2:1; 5% biocatalyst (*w/w*).

The BCL, like most lipases, is characterized by the presence of a catalytic triad made up of Ser87, Asp264, and His286 residues together with a mobile lid domain located over their catalytic triad, which rearranges at the oil–water interface [40–42].

Recent research showed that the preference of BCL for the catalysis of triacylglycerol and carboxylic acid molecules, could be elucidated by molecular docking analysis [43–46]. By analyzing the efficiency of BCL in the transesterification of coconut oil and its interactions with molecules of mono-, di-, and triacylglycerol, Santana et al., 2020 [43] highlighted the importance of molecular docking to explain lipases preference for attacking toward a given position in the backbone of triacylglycerol, which results in the formation of intermediate and final products of the transesterification reaction. Results showed that the interaction between amino acid residues in the active site of BCL (Ser87 and His286) and triacylglycerol is preferred, which explained the low levels of monoacylglycerol conversion in the first 48 h of reaction [43].

Thus, in order to understand at the molecular level this preferential attack of BCL toward given specific molecules of acidolysis substrate, interactions between the three-dimensional structure of BCL (PDB: 3LIP) with oleic acid or tripalmitin molecules were evaluated by molecular docking. Therefore, it was possible to identify the specific interactions, types of interactions, lowest absolute affinity values (kcal/mol), and geometrical distances (Å), as well as the molecular interaction diagrams between the amino acids of BCL with oleic acid or tripalmitin molecules (data reported in supplementary materials (Table S1 and Figures S1 and S2)). The absolute values of affinity and docking poses for each ligand in BCL are displayed in Figure 6. The molecular docking results indicate that both oleic acid and tripalmitin interact within the active site. The preferred binding site lies at the amino acid residue His286 and is stabilized by hydrophobic interactions. However, the preference attack of BCL can also be evaluated through the docking affinity energy values with oleic acid or tripalmitin molecules. The ligands oleic acid and tripalmitin have high binding energies with BCL, namely -6.5 and -5.4 kcal·mol⁻¹, respectively. The lower the affinity energy values (or the higher their absolute values), the higher is the interaction energy between the ligand and the enzyme. Thus, oleic acid with lower affinity energy value has a higher preference to interact with the BCL. This might be the reason why the reaction period was long, due to the greater preference of BCL for catalyzing oleic acid. The attack on tripalmitin and subsequent formation of the HMFS only occur after the catalysis of most oleic acid molecules.

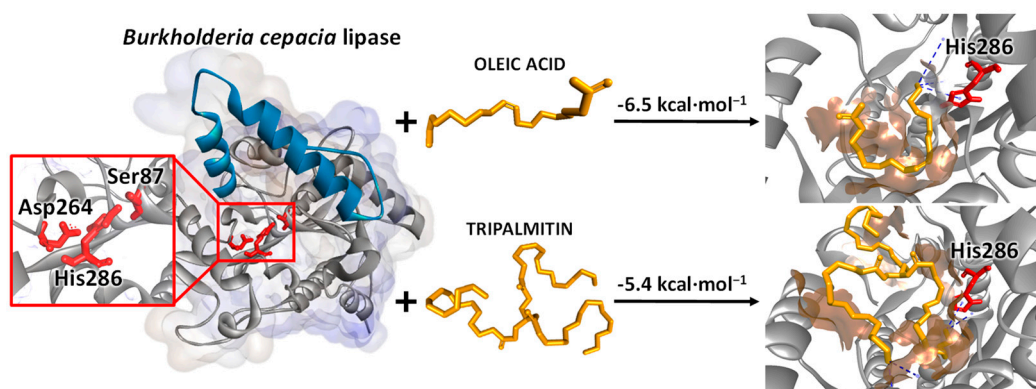


Figure 6. Molecular docking and affinities between BCL (PDB: 3LIP) and oleic acid, or tripalmitin (shown in orange). BCL catalytic triad is shown in red (Ser87, Asp264, and His286) and lid domain in blue (amino acids residues between Glu118 and Asp159). The specific interactions are indicated as ---.

2.4. Optimization of the Enzymatic Acidolysis

In order to develop an acidolysis process with a high yield for the oleic acid incorporation, the influence of reaction temperature (T) and molar ratio (MR) were evaluated. The enzyme loading in the support was maintained constant at 5% (*w/w* of tripalmitin) according to the amount used in similar studies [14,15,31]. The results of the set of 11 experiments of the CCRD are presented in Table 1.

Table 1. Central composite rotatable design (CCRD) followed in the experiments as a function of temperature (T) and the molar ratio oleic acid: tripalmitin (MR) and respective values of oleic acid incorporation, after 48 h reaction, catalyzed by C-AIL biocatalyst.

Data Set	Experiments	Coded Matrix		Decoded Matrix		Oleic Acid Incorporation (mol.%)
		T (°C)	MR	T (°C)	MR	
Full factorial points	1	−1	−1	60	2:1	23.5
	2	−1	1	60	6:1	11.0
	3	1	−1	70	2:1	17.0
	4	1	1	70	6:1	6.3
Star-points	5	−1.41	0	58	4:1	27.6
	6	1.41	0	72	4:1	8.6
	7	0	−1.41	65	1.2:1	3.7
	8	0	1.41	65	6.8:1	6.3
Center points	9	0	0	65	4:1	16.2
	10	0	0	65	4:1	15.7
	11	0	0	65	4:1	16.4

The linear and quadratic effects of T and MR, as well as the interaction effects, and respective *p*-values, were calculated using the experimental results. It can be seen from Table 2 that temperature (linear term) was the most significant independent factor, followed by MR (quadratic term). Both temperature (linear term) and substrate molar ratio (linear term) have negative effects on the response. Thus, lower temperature and MR values promote oleic acid incorporation. The negative quadratic effect of MR shows that incorporation is described by a convex surface as a function of MR. No significant effect of the interaction of T with MR was observed.

Table 2. Linear and quadratic effects of temperature (T) and molar ratio (MR) of oleic acid/tripalmitin, linear interaction T × MR, and respective *p*-values, on the values of oleic acid incorporation (mol.%), after 48 h acidolysis, catalyzed by C-AIL biocatalyst.

Factor	Effect	<i>p</i> -Value
T (linear term)	−9.54	0.051
T (quadratic term)	3.62	0.458
MR (linear term)	−4.95	0.244
MR (quadratic term)	−9.80	0.082
T × MR	0.895	0.872

The analysis of variance (ANOVA) of the regression model considering all the linear, quadratic, and interaction terms, is shown in Table 3. The F-test, together with the *p*-value, the coefficient of determination (R^2), and adjusted R^2 , were used to assess the statistical significance of the second-order polynomial model and the fit of the model to the experimental results. Table 3 shows that the calculated F value (F_{calc}) is equal to 5.27, which is larger than the F critical value (4.06); the *p*-value is very small (0.00005), indicating a low probability of error value; and the determination coefficient (R^2) and adjusted R^2 are equal to 0.752 and 0.504, respectively. These statistical parameters indicate a good fit of the second-order polynomial model to the experimental data.

Table 3. ANOVA for the results of non-linear RSM model.

Variation Source	Sum of Squares	Degree of Freedom	Mean Square	F_{calc}	<i>p</i> -Value
Regression	378.29	10	37.83	5.27	0.00005
Residuals	43.09	6	7.18		
Lack of Fit	560.27	1	560.27		
Pure Error	138.89	5	27.78		
Total	560.27	16			

However, the values of R^2 and adjusted R^2 are quite different from each other, indicating that non-significant factor terms were considered. Therefore, to improve the fit of the model, the quadratic effect of temperature and the linear interaction between temperature and MR ($p \gg 0.05$) were removed from the model. Only the factors with significant effects ($p \leq 0.05$), or those whose removal would lead to a lack of fit of the model, were retained. Moreover, according to Haaland (1989) [30], the practical significance of a factor may be not coincident with its statistical significance.

Thus, oleic acid incorporation values (mol.%) can be fitted to a three-dimensional convex surface (Figure 7) described by a second-order polynomial model as a function of T (°C) and MR oleic acid/tripalmitin (Equation (1)):

$$\text{Inc. values (mol.\%)} = 63.03 - 0.954 T + 9.59 MR - 1.35 MR^2 \quad (1)$$

The values obtained for R^2 and adjusted R^2 of this model were 0.73 and 0.60, respectively. This indicates that 73% of experimental data are explained by this model, suggesting a close agreement between the experimental data and the theoretical values predicted by the model. The value of R^2 is lower than the desirable minimum of 0.75 suggested by Haaland (1989) [30]. It is possible that the activity of the biocatalyst used in each experiment will not be the same for all the CCRD experiments. In fact, during immobilization, a lack of homogeneous distribution of enzyme molecules in the support, together with eventual stereochemical and conformational phenomena, may occur, explaining the variability in enzyme activity and, consequently, a lower fit of the model.

Temperature is a limiting variable in this process since it is necessary to ensure values equal or higher than 58 °C to prevent medium solidification. In addition, higher temperatures resulted in lower oleic acid incorporations. Therefore, it is necessary to select a

suitable temperature to guarantee the high rate of acidolysis reaction and, at the same time, to reduce a possible inactivation of the biocatalyst at high temperature. For a temperature of 58 °C, an incorporation level of oleic acid of about 28 mol.% was observed (Table 1) when oleic acid was used in stoichiometric excess (MR 4:1). This value is not very much different from the value obtained with the stoichiometric MR of 2:1 (27.6 mol.%). Therefore, to lower reaction costs, the use of lower MR is preferred.

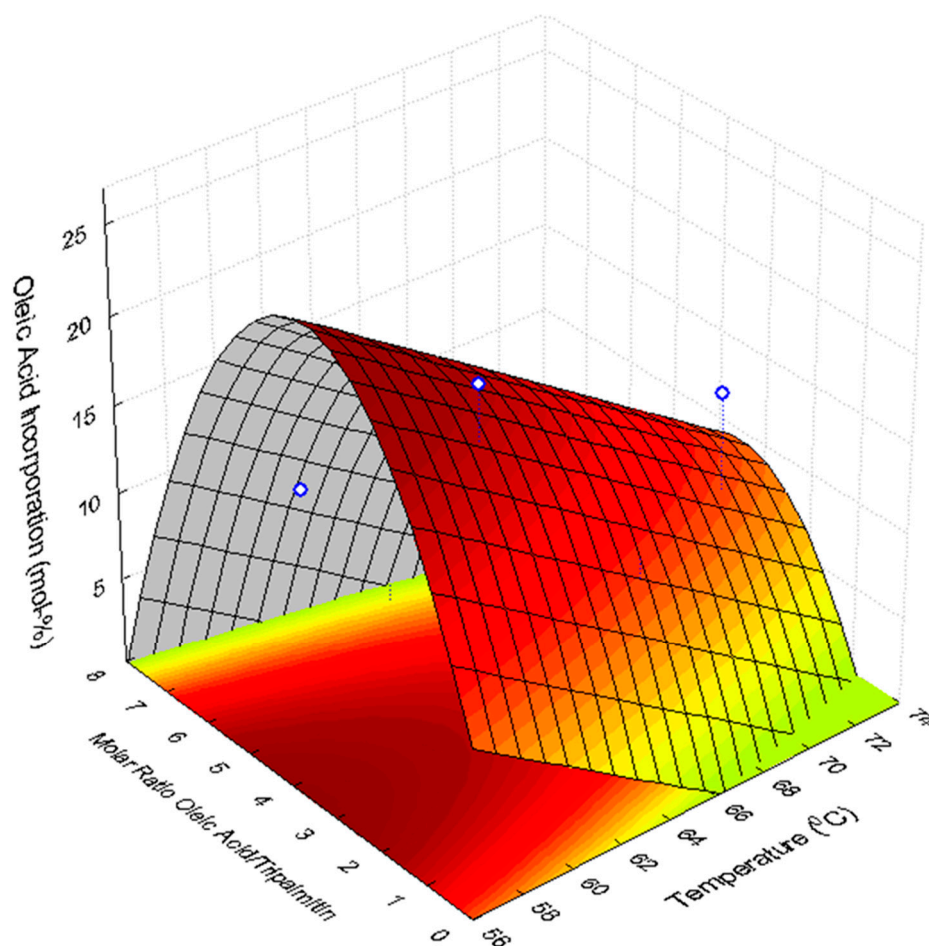


Figure 7. Response surface fitted to the oleic acid incorporation values as a function of temperature and substrate molar ratio (oleic acid: tripalmitin), after 48 h acidolysis catalyzed by C-AIL.

Similar levels for oleic acid incorporation in tripalmitin were attained in previous studies using *Carica papaya* lipase self-immobilized in papaya latex, under similar reaction conditions [14,47]. Wei et al. (2015) [1] established a method of producing OPO in two steps: (i) synthesis of tripalmitin by interesterification of PA with glycerol using NaOH as catalyst, followed by (ii) acidolysis of tripalmitin with oleic acid in solvent (*n*-hexane) and solvent-free media catalyzed by the commercial immobilized lipases Lipozyme TL IM (*Thermomyces lanuginosus* lipase) and Lipozyme RM IM (*Rhizomucor miehei* lipase). In the solvent-free system, the highest OPO content (40.23%) was achieved for Lipozyme RM IM (12% of total substrate weight) at higher temperature (60 °C) and molar ratio 6:1 (oleic acid/PPP) than those used in the present study [1].

Recently, an improved OPO content (46.5%) was reached using *Candida lipolytica* lipase immobilized on magnetic multi-walled carbon nanotubes in the acidolysis reaction between tripalmitin and oleic acid under optimized conditions (2% water, 20% enzyme, MR of 6:1 oleic acid/tripalmitin, 50 °C) [48]. Nevertheless, both high FFA content in the reaction media and high enzyme loads used in these studies, increase enzyme and downstream costs required for recycling unconverted substrates and for product recovery. It is worth

mentioning that in our study, a biocatalyst load of 5% of the weight of tripalmitin was used, and 58 °C and a ratio oleic acid/tripalmitin of 4:1 (or 2:1) were found as the best reaction conditions.

3. Materials and Methods

3.1. Materials

The *Burkholderia cepacia* lipase (BCL) was purchased from Sigma-Aldrich (Tokyo, Japan). The silane precursor tetraethoxysilane (TEOS) was supplied by Acros Organic (Morris Plains, NJ, USA) and used without further purification; γ -triethoxysilylpropylamine (γ -APTS) was obtained from Sigma-Aldrich (St. Louis, MO, USA). Ethanol, ammonia, hydrochloric acid, and gum arabic were obtained from Synth (São Paulo, Brazil); tripalmitin (>85% purity; M.W. = 807.35 g·mol⁻¹) was obtained from TCI Europe; 2',7'-dichlorofluorescein was obtained from Fluka; and extra pure oleic acid (M.W. = 282.5 g·mol⁻¹), Silica-Gel 60 (0.25 mm width, 20 × 20 cm) thin layer chromatography (TLC) plates, and glutaraldehyde (25% aqueous solution) were purchased from Merck (Burlington, MA, USA). Extra virgin olive oil was purchased in a local Portuguese market. Water was purified by reverse osmosis and deionized through a Milli-Q four-cartridge organic-free water purification system. The ionic liquids used were: 1-butyl-3-methylimidazolium bis(trifluoromethylsulfonyl) imide ([C₄mim][NTf₂], aprotic IL named AIL in this manuscript), obtained from Fluka; and N-methylmonoethanolamine pentanoate (protic IL named PIL in this manuscript), supplied by the Universidade Federal da Bahia (UFBA), Brazil. The other chemicals were of analytical grade and were used as received.

3.2. BCL Immobilization by Covalent Binding and Encapsulation

A methodology previously established by Souza et al., 2013 [29] was used for lipase immobilization, and it is briefly described as follows: 30 mL of TEOS were dissolved in 36 mL of absolute ethanol under inert nitrogen atmosphere. To this solution, 0.22 mL of hydrochloric acid dissolved in 5 mL ultra-pure water was added, and the mixture was stirred (200 rpm) for 90 min at 35 °C. For encapsulation, the BCL (870.71 U) was solubilized in 10 mL of water and 1% (*w/v*) of the ILs (AIL or PIL) were added. Next, 1.0 mL of ammonium hydroxide solubilized in 6.0 mL of ethanol (hydrolysis solution) was added to the sol-gel reaction medium. The mixture was kept under static conditions for 24 h to complete polycondensation. The bulk gel was then washed with heptane and acetone (3 times with 30 mL of each solvent) and dried under reduced pressure at 25 °C for 72 h. These biocatalysts will be called E-AIL and E-PIL.

For covalent binding immobilization, the silica was subsequently silanized with γ -APTS followed by the activation reaction with glutaraldehyde solution, and then the lipase was immobilized by covalent binding according to the procedure described by Soares et al., 2004 [38]. These biocatalysts will be called C-AIL or C-PIL throughout this manuscript.

3.3. Morphological and Physicochemical Properties

The samples of pure silica and free and immobilized lipase in the absence or in the presence of the additive, were submitted to FTIR analysis (spectrophotometer FTIR BOMEMMB-100, ABB-Bomem, Quebec, QC, Canada). Amounts of approximately 6 mg of the solid were used for sample characterization. The spectral information was obtained in a range between 500 and 4000 cm⁻¹ with a resolution of 4 cm⁻¹ and 32 scans. Thermogravimetric curves were obtained using a Shimadzu DTG-60H Simultaneous DTA-TG apparatus, under a nitrogen atmosphere. The analysis started at 25 °C and increased up to 1000 °C, at a rate of 20 °C·min⁻¹, using around 30–50 mg of the samples. Scanning electron microscopy (SEM; model Hitachi SU-70) was used to characterize the surfaces of the supports, the free lipase, and the immobilized lipase preparations.

3.4. Synthesis of HMFS by Enzymatic Acidolysis

Acidolysis reactions were performed batch-wise in closed thermostated cylindrical batch reactors (20 mL). A load of 5% (*w/w* of tripalmitin) of immobilized enzyme was added to the reaction medium, after complete melting of tripalmitin. This load is currently used in interesterification experiments without problems of mass transfer limitation [13,14]. Reactions were performed at 60 °C unless otherwise stated. Prior to and at different reaction times, 1 mL samples were taken, and the biocatalyst was removed by paper filtration at approximately 70 °C. All samples were stored at −18 °C for subsequent analysis. The molar ratio oleic acid/tripalmitin was set at 2:1 for the screening and time-course experiments, which is the stoichiometric value for the reaction. In optimization studies, MR varied according to the experimental design. All the experiments were carried out in triplicate. Molar incorporation degree (%) was calculated based on the molecular weight of oleic acid (282.5 g·mol^{−1}).

3.5. Experimental Design Experiments

Response surface methodology (RSM) was used to model and optimize the reaction conditions. The central composite rotatable design (CCRD) is one of the most used experimental designs in RSM. In this design, each factor (variable) is tested at five different levels, allowing the fitting of curved surfaces, described by second order polynomials, to the experimental data. The coefficients of these equations are usually unknown. Therefore, their estimates are obtained by the statistical principle of least squares applied to the experimental data. A CCRD is a matrix consisting of 3 sets of experiments, as a function of *k* factors: a full factorial design with 2^{*k*} experiments (coded levels −1 and +1); a set of 2*k* axial or star-points outside the factorial matrix, but inside the experimental domain at a distance 2^{*k*/4} from the origin; and a set of center points, which are located at the origin of the system (coded level = 0). The repetition of the center points will provide an estimate of the variance of the experimental error, which is assumed to be constant along the experimental domain [30,49].

Therefore, the acidolysis experiments were carried out following a CCRD, as a function of 2 factors: temperature (*T*: 58–72 °C), and reaction medium formulation (molar ratio oleic acid/tripalmitin: 1.2:1–6.8:1) (Table 1). The temperature of 72 °C is the alpha value (star value) for the temperature, corresponding to a coded value of $\sqrt{2} \approx 1.41$, while the lowest temperature tested was 58 °C, corresponding to the coded value of $-\alpha$, which is equal to approximately −1.41. For molar ratio (MR), the decoded alpha values were 6.8:1 and 1.2:1, respectively (positive and negative coded values). A total of 11 assays with 3 replicates of the center point (65 °C; MR = 4:1) were generated. Experiments were conducted randomly, according to the methodology described for acidolysis reaction. The minimum temperature tested was dictated by the melting point of the reaction media (melting point of tripalmitin = 66 °C). After 48 h reaction, the medium was separated from the enzyme by paper filtration in an oven at approximately 70 °C, and stored at −18 °C for subsequent analysis.

3.6. Evaluation of Incorporation Degree

The amount of oleic acid incorporated in TAG was determined according to Tecelão et al. [13], as briefly described: a solution of the reaction medium in chloroform was spotted on a continuous layer on a silica gel TLC plate. After elution, the plate was sprayed with 2',7'-dichlorofluorescein and observed under UV light. The various groups of compounds (TAG, free fatty acids, diacylglycerols, and monoacylglycerols) were identified by comparison with standards. The TAG band was scraped off and methylated, to be assayed as fatty acid methyl esters (FAME) by GC. FAME were dissolved in 100 µL of *n*-hexane, and 1 µL was analyzed in a Finnigan TRACE GC Ultra gas chromatograph (Thermo Electron Corporation, Waltham, MA, USA) equipped with a Thermo TR-FAME capillary column (30 m × 0.25 mm ID × 0.25 mm film), an auto sampler AS 3000 from Thermo Fisher Scientific (Waltham, MA, USA), and a FID detector. Injector (in splitless mode) and detector temperatures were set at 250 and 260 °C, respectively. Helium was

used as the carrier gas at a flow rate of $1.5 \text{ mL}\cdot\text{min}^{-1}$. Air and hydrogen were supplied to the detector at flow rates of 350 and $35 \text{ mL}\cdot\text{min}^{-1}$, respectively. For the analysis of samples, the oven temperature program was as follows: $60 \text{ }^\circ\text{C}$ for 1 min , a temperature increase to $150 \text{ }^\circ\text{C}$ at $15 \text{ }^\circ\text{C}\cdot\text{min}^{-1}$, a plateau at $150 \text{ }^\circ\text{C}$ for 1 min , followed by temperature increase to $180 \text{ }^\circ\text{C}$ at $5 \text{ }^\circ\text{C}\cdot\text{min}^{-1}$, a plateau at $180 \text{ }^\circ\text{C}$ for 3 min , an increase in temperature until $220 \text{ }^\circ\text{C}$, at a rate of $10 \text{ }^\circ\text{C}\cdot\text{min}^{-1}$, and a final plateau at $220 \text{ }^\circ\text{C}$ for 1 min .

The incorporation degree (w%) of oleic acid in the triacylglycerols was calculated as the ratio between the peak area of methyl oleate and the sum of areas of methyl oleate and methyl palmitate peaks in the chromatogram. To obtain the mole % incorporation value, the number of moles of methyl oleate and methyl palmitate were calculated using the respective molar weights. Finally, the molar incorporation of oleic acid was obtained by dividing the number of moles of methyl oleate by the total number of moles (methyl oleate and methyl palmitate).

3.7. Molecular Docking Analysis

The interactions of BCL (receptor) with the oleic acid and tripalmitin (ligands) were identified using the AutoDock Vina 1.1.2 program [50]. The crystal structure of BCL (PDB: 3lip) was downloaded and applied for molecular docking. AutoDockTools (ADT) [51] was used to prepare the BCL input file by merging non-polar hydrogen atoms, adding partial charges, and atom types. Ligands 3D (oleic acid and tripalmitin) atomic coordinates were downloaded from the ZINC database (zinc.docking.org, accessed on 23 March 2023), and the ligand rigid root was generated using AutoDockTools (ADT), setting all possible rotatable bonds defined as active by torsions. The grid centers at the centers of mass of BCL were $7.348 \times 0.532 \times 17.922 \text{ \AA}$, and $56 \times 58 \times 58 \text{ \AA}$ in the x-, y-, and z-axes, respectively.

The binding model that has the lowest binding free energy was searched out from 10 different conformers for each ligand. The complexes of BCL and oleic acid and tripalmitin were visualized and analyzed using Discovery Studio, v20 (Accelrys, San Diego, CA, USA).

3.8. Statistical Analysis

The software Statistica[®], version 7.0, Tulsa, OK, USA, was used for: (i) the one-way analysis of variance (ANOVA; Tukey test, $p \leq 0.05$) of the results of hydrolytic and acidolysis activity of the different lipase preparations; and (ii) to analyze the results of the CCRD concerning oleic acid incorporation in TAG. Both linear and quadratic effects of each factor under study (temperature and oleic acid: tripalmitin molar ratio), as well as their linear interaction, on acidolysis reaction, were calculated. Their significance was evaluated by ANOVA. A three-dimensional surface, described by a second-order polynomial equation, was fitted to the experimental values of the CCRD, as a function of temperature and MR (Table 1). First and second-order coefficients of this equation were estimated from the experimental data using the statistical principle of least squares. The goodness of fit of the model was evaluated by the determination coefficient (R^2) and adjusted R^2 (R^2_{adj}). The R^2 is calculated by the ratio between the variation explained by the model and the total variation of the experimental data. Its value provides a measure of how much of the variability in the observed response values can be explained by the experimental factors and their interactions. R^2_{adj} is an unbiased estimate of the coefficient of determination, because it corrects the R^2 value for the sample size and the number of terms in the model. It is always smaller than R^2 . High values of both R^2 and R^2_{adj} suggest a good fit of the model to the experimental data. In practice, R^2 should be at least 0.75 or greater; values above 0.90 are very good [30].

4. Conclusions

This study shows the potential of BCL immobilized by covalent binding or encapsulation in silica prepared with ILs, as biocatalyst for the production of HMFS. The highest incorporation of oleic acid in tripalmitin was attained with BCL immobilized by covalent binding in silica prepared with AIL. The molecular docking analysis provided important

information on the BCL specificity for specific molecules of acidolysis substrates (oleic acid and tripalmitin). Thereby, it elucidated the long reaction time required for the incorporation of oleic acid in tripalmitin, since BCL has a higher preference to interact with oleic acid than with tripalmitin. According to the RSM used to model and optimize operation conditions, an incorporation level of oleic acid of about 28%-mol is achieved at 58 °C and an MR of 4:1 (oleic acid: tripalmitin) after 48 h reaction, using a biocatalyst load of 5% (*w/w*). Since similar incorporations were found using an MR of 2:1 and 60 °C, these conditions should be selected to lower substrate costs. Therefore, the synthesis of all this information allows for the rational design of efficient and sustainable HMFS production.

Supplementary Materials: The following supporting information can be downloaded at: <https://www.mdpi.com/article/10.3390/catal13050825/s1>, Figure S1: Molecular interaction diagrams of *Burkholderia cepacia* lipase (BCL) with oleic acid.; Figure S2: Molecular interaction diagrams of *Burkholderia cepacia* lipase (BCL) with tripalmitin; Table S1: Docking affinity energy and interactions of molecules individually with amino acids of *Burkholderia cepacia* lipase (BCL), predicted by AutoDock Vina.

Author Contributions: Conceptualization: S.F.-D., C.T. and C.M.F.S.; methodology: S.B.S., C.T. and S.M.; software, M.S.B. and M.M.P.; validation: C.M.F.S., Á.S.L. and S.F.-D.; formal analysis: S.F.-D.; investigation: C.M.F.S. and C.T.; resources: C.M.F.S. and S.F.-D.; data curation, C.M.F.S., C.T. and S.F.-D.; writing—original draft preparation: C.M.F.S., M.S.B. and M.M.P.; writing—review and editing: S.F.-D.; visualization, C.T.; supervision, S.F.-D.; project administration: S.F.-D.; funding acquisition: S.F.-D. All authors have read and agreed to the published version of the manuscript.

Funding: This research was funded by (i) Coordenação de Aperfeiçoamento de Pessoal de Ensino Superior (CAPES) and Conselho Nacional de Desenvolvimento Científico e Tecnológico (CNPq), Brazil, (ii) the national funding of FCT-Fundação para a Ciência e a Tecnologia (FCT), Portugal, to the research units LEAF—Linking Landscape, Environment, Agriculture and Food Research Centre (UIDB/04129/2020; UIDP/04129/2020), MARE (UIDB/04292/2020; UIDP/04292/2020), CIEPQPF (UIDB/EQU/00102/2020 and UIDP/EQU/00102/2020) and (iii) to the project LA/P/0069/2020 granted to the Associate Laboratory ARNET.

Data Availability Statement: Data is available from the authors upon request.

Conflicts of Interest: The authors declare no conflict of interest.

References

1. Wei, W.; Yongfang, F.; Zhang, X.; Cao, X.; Feng, F. Synthesis of Structured Lipid 1,3-Dioleoyl-2-Palmitoylglycerol in Both Solvent and Solvent-Free System. *LWT-Food Sci. Technol.* **2015**, *12*, 1187–1194. [[CrossRef](#)]
2. Ferreira-Dias, S.; Osório, N.M.; Rodrigues, J.; Tecelão, C. Structured Lipids for Foods. In *Encyclopedia of Food Chemistry*; Elsevier: Amsterdam, The Netherlands, 2019; Volume 3, pp. 357–369. ISBN 2050011504.
3. Ferreira-Dias, S.; Osório, N.; Tecelão, C. Bioprocess Technologies for Production of Structured Lipids as Nutraceuticals. In *Current Developments in Biotechnology and Bioengineering*; Elsevier: Amsterdam, The Netherlands, 2022; Volume 2, pp. 209–237, ISBN 9780128235065.
4. Ferreira-Dias, S.; Tecelão, C. Human Milk Fat Substitutes: Advances and Constraints of Enzyme-Catalyzed Production. *Lipid Technol.* **2014**, *26*, 183–186. [[CrossRef](#)]
5. Şahin-Yeşilçubuk, N.; Akoh, C.C. Biotechnological and Novel Approaches for Designing Structured Lipids Intended for Infant Nutrition. *JAACS J. Am. Oil Chem. Soc.* **2017**, *94*, 1005–1034. [[CrossRef](#)]
6. Wei, W.; Jin, Q.; Wang, X. Human Milk Fat Substitutes: Past Achievements and Current Trends. *Prog. Lipid Res.* **2019**, *74*, 69–86. [[CrossRef](#)]
7. Annapure, U.S.; Jadhav, H.B. A Brief Overview on the Role of Human Milk Fat Substitutes in the Growth of Infants. 2022. Available online: <https://www.foodinfotech.com/role-of-human-milk-fat-substitutes-in-the-growth-of-infants-an-overview/> (accessed on 23 March 2023).
8. Jiang, X.; Zou, X.; Chao, Z.; Xu, X. Preparation of Human Milk Fat Substitutes: A Review. *Life* **2022**, *12*, 187. [[CrossRef](#)]
9. Liu, Z.; Dai, L.; Liu, D.; Du, W. Progress and Perspectives of Enzymatic Preparation of Human Milk Fat Substitutes. *Biotechnol. Biofuels Bioprod.* **2022**, *15*, 118. [[CrossRef](#)]
10. Mu, H. Production and Nutritional Aspects of Human Milk Fat Substitutes. *Lipid Technol.* **2010**, *22*, 126–129. [[CrossRef](#)]
11. Ghide, M.K.; Yan, Y. 1,3-Dioleoyl-2-Palmitoyl Glycerol (OPO)—Enzymatic Synthesis and Use as an Important Supplement in Infant Formulas. *J. Food Biochem.* **2021**, *45*, e13799. [[CrossRef](#)]

12. Robles, A.; Jiménez, M.J.; Esteban, L.; González, P.A.; Martín, L.; Rodríguez, A.; Molina, E. Enzymatic Production of Human Milk Fat Substitutes Containing Palmitic and Docosahexaenoic Acids at Sn-2 Position and Oleic Acid at Sn-1,3 Positions. *LWT-Food Sci. Technol.* **2011**, *44*, 1986–1992. [CrossRef]
13. Tecelão, C.; Silva, J.; Dubreucq, E.; Ribeiro, M.H.; Ferreira-Dias, S. Production of Human Milk Fat Substitutes Enriched in Omega-3 Polyunsaturated Fatty Acids Using Immobilized Commercial Lipases and *Candida parapsilosis* Lipase/Acyltransferase. *J. Mol. Catal. B Enzym.* **2010**, *65*, 122–127. [CrossRef]
14. Tecelão, C.; Rivera, I.; Sandoval, G.; Ferreira-Dias, S. *Carica papaya* Latex: A Low-Cost Biocatalyst for Human Milk Fat Substitutes Production. *Eur. J. Lipid Sci. Technol.* **2012**, *114*, 266–276. [CrossRef]
15. Simões, T.; Valero, F.; Tecelão, C.; Ferreira-Dias, S. Production of Human Milk Fat Substitutes Catalyzed by a Heterologous *Rhizopus oryzae* Lipase and Commercial Lipases. *JAOCS J. Am. Oil Chem. Soc.* **2014**, *91*, 411–419. [CrossRef]
16. Tecelão, C.; Perrier, V.; Dubreucq, E.; Ferreira-Dias, S. Production of Human Milk Fat Substitutes by Interesterification of Tripalmitin with Ethyl Oleate Catalyzed by *Candida parapsilosis* Lipase/Acyltransferase. *JAOCS J. Am. Oil Chem. Soc.* **2019**, *96*, 777–787. [CrossRef]
17. Available online: <https://europe.bungeloders.com/en/brand/betapol-3> (accessed on 23 March 2023).
18. Available online: <https://advancedlipids.com/products/> (accessed on 23 March 2023).
19. Available online: <https://www.wilmar-international.com/specialty-fats/products/nutritional-lipids> (accessed on 23 March 2023).
20. Sheldon, R.A.; van Pelt, S. Enzyme Immobilisation in Biocatalysis: Why, What and How. *Chem. Soc. Rev.* **2013**, *42*, 6223–6235. [CrossRef]
21. Barbosa, M.; Santos, A.; Carvalho, N.B.; Figueiredo, R.; Pereira, M.M.; Lima, Á.S.; Freire, M.G.; Cabrera-Padilla, R.; Soares, C.M.F. Enhanced Activity of Immobilized Lipase by Phosphonium-Based Ionic Liquids Used in the Supports Preparation and Immobilization Process. *ACS Sustain. Chem. Eng.* **2019**, *7*, 15648–15659. [CrossRef]
22. da Silva, V.G.; de Castro, R.J.S. Biocatalytic Action of Proteases in Ionic Liquids: Improvements on Their Enzymatic Activity, Thermal Stability and Kinetic Parameters. *Int. J. Biol. Macromol.* **2018**, *114*, 124–129. [CrossRef]
23. Barbosa, M.S.; Freire, C.C.C.; Souza, R.L.; Cabrera, R.Y. Effects of Phosphonium-Based Ionic Liquids on the Lipase Activity Evaluated by Experimental Results and Molecular Docking. *Biotechnol. Prog.* **2019**, *35*, e2816. [CrossRef] [PubMed]
24. Cull, S.G.; Holbrey, J.D.; Vargas-Mora, V.; Seddon, K.R.; Lye, G.J. Room-Temperature Ionic Liquids as Replacements for Organic Solvents in Multiphase Bioprocess Operations. *Biotechnol. Bioeng.* **2000**, *69*, 227–233. [CrossRef]
25. Rebelo, L.P.N.; Lopes, N.C.; Esperanc, M.S.S. On the Critical Temperature, Normal Boiling Point, and Vapor Pressure of Ionic Liquids. *J. Phys. Chem. B* **2005**, *109*, 6040–6043. [CrossRef]
26. Welton, T. Room-Temperature Ionic Liquids. Solvents for Synthesis and Catalysis. *Chem. Rev.* **1999**, *99*, 2071–2084. [CrossRef]
27. Toledo Hijo, A.A.C.; Maximo, G.J.; Costa, M.C.; Batista, E.A.C.; Meirelles, A.J.A. Applications of Ionic Liquids in the Food and Bioproducts Industries. *ACS Sustain. Chem. Eng.* **2016**, *4*, 5347–5369. [CrossRef]
28. Deetlefs, M.; Seddon, K.R.; Seddon, K. Assessing the Greenness of Some Typical Laboratory Ionic Liquid Preparations. *Green Chem.* **2010**, *12*, 17–30. [CrossRef]
29. Souza, R.L.; Faria, E.L.P.; Figueiredo, R.T.; Freitas, L.S.; Iglesias, M.; Mattedi, S.; Zanin, G.M.; Dos Santos, O.A.A.; Coutinho, J.A.P.; Lima, A.S.; et al. Protic Ionic Liquid as Additive on Lipase Immobilization Using Silica Sol-Gel. *Enzyme Microb. Technol.* **2013**, *52*, 141–150. [CrossRef] [PubMed]
30. Haaland, P.D. *Experimental Design in Biotechnology, Statistics: Textbooks and Monographs*; CRC Press: Boca Raton, FL, USA, 1989; Volume 1, ISBN 0824778812.
31. Faustino, A.R.; Osório, N.M.; Tecelão, C.; Canet, A.; Valero, F.; Ferreira-Dias, S. Camelina Oil as a Source of Polyunsaturated Fatty Acids for the Production of Human Milk Fat Substitutes Catalyzed by a Heterologous *Rhizopus oryzae* Lipase. *Eur. J. Lipid Sci. Technol.* **2016**, *118*, 532–544. [CrossRef]
32. Carvalho, N.B.; Vidal, B.T.; Barbosa, A.S.; Pereira, M.M.; Mattedi, S.; Freitas, L.D.S.; Lima, Á.S.; Soares, C.M.F. Lipase Immobilization on Silica Xerogel Treated with Protic Ionic Liquid and Its Application in Biodiesel Production from Different Oils. *Int. J. Mol. Sci.* **2018**, *19*, 1829. [CrossRef]
33. Portaccio, M.; Della Ventura, B.; Mita, D.G.; Manolova, N.; Stoilova, O.; Rashkov, I.; Lepore, M. FT-IR Microscopy Characterization of Sol-Gel Layers Prior and after Glucose Oxidase Immobilization for Biosensing Applications. *J. Sol-Gel Sci. Technol.* **2011**, *57*, 204–211. [CrossRef]
34. Hu, Y.; Tang, S.; Jiang, L.; Zou, B.; Yang, J.; Huang, H. Immobilization of *Burkholderia cepacia* Lipase on Functionalized Ionic Liquids Modified Mesoporous Silica SBA-15. *Process Biochem.* **2012**, *47*, 2291–2299. [CrossRef]
35. You, P.; Su, E.; Yang, X.; Mao, D.; Wei, D. *Carica papaya* Lipase-Catalyzed Synthesis of Terpene Esters. *J. Mol. Catal. B Enzym.* **2011**, *71*, 152–158. [CrossRef]
36. Mukherjee, I.; Mylonakis, A.; Guo, Y.; Samuel, S.P.; Li, S.; Wei, R.Y.; Kojtari, A.; Wei, Y. Effect of Nonsurfactant Template Content on the Particle Size and Surface Area of Monodisperse Mesoporous Silica Nanospheres. *Microporous Mesoporous Mater.* **2009**, *122*, 168–174. [CrossRef]
37. Wei, Y.; Xu, J.; Dong, H.; Dong, J.H.; Qiu, K.; Jansen-Varnum, S.A. Preparation and Physisorption Characterization of D-Glucose-Templated Mesoporous Silica Sol-Gel Materials. *Chem. Mater.* **1999**, *11*, 2023–2029. [CrossRef]
38. Soares, C.M.F.; Dos Santos, O.A.; De Castro, H.F.; De Moraes, F.F.; Zanin, G.M. Studies on Lipase Immobilization in Hydrophobic Sol-Gel Matrix. *Appl. Biochem. Biotechnol.* **2004**, *113*, 307–319. [CrossRef] [PubMed]

39. Zou, B.; Song, C.; Xu, X.; Xia, J.; Huo, S.; Cui, F. Enhancing Stabilities of Lipase by Enzyme Aggregate Coating Immobilized onto Ionic Liquid Modified Mesoporous Materials. *Appl. Surf. Sci.* **2014**, *311*, 62–67. [[CrossRef](#)]
40. Khan, F.I.; Lan, D.; Durrani, R.; Huan, W.; Zhao, Z.; Wang, Y. The Lid Domain in Lipases: Structural and Functional Determinant of Enzymatic Properties. *Front. Bioeng. Biotechnol.* **2017**, *5*, 16. [[CrossRef](#)] [[PubMed](#)]
41. Sánchez, D.A.; Tonetto, G.M.; Ferreira, M.L. *Burkholderia cepacia* Lipase: A Versatile Catalyst in Synthesis Reactions. *Biotechnol. Bioeng.* **2018**, *115*, 6–24. [[CrossRef](#)] [[PubMed](#)]
42. Barbe, S.; Lafaquière, V.; Guieysse, D.; Monsan, P.; Remaud-Siméon, M.; André, I. Insights into Lid Movements of *Burkholderia cepacia* Lipase Inferred from Molecular Dynamics Simulations. *Proteins Struct. Funct. Bioinform.* **2009**, *77*, 509–523. [[CrossRef](#)] [[PubMed](#)]
43. Santana, J.L.; Oliveira, J.M.; Nascimento, J.S.; Mattedi, S.; Krause, L.C.; Freitas, L.S.; Cavalcanti, E.B.; Pereira, M.M.; Lima, A.S.; Soares, C.M.F. Continuous Flow Reactor Based with an Immobilised Biocatalyst for the Continuous Enzymatic Transesterification of Crude Coconut Oil. *Biotechnol. Appl. Biochem.* **2020**, *55*, 404–413. [[CrossRef](#)]
44. Barbosa, M.S.; Freire, C.C.C.; Almeida, L.C.; Freitas, L.S.; Souza, R.L.; Pereira, E.B.; Mendes, A.A.; Pereira, M.M.; Lima, Á.S.; Soares, C.M.F. Optimization of the Enzymatic Hydrolysis of *Moringa oleifera* Lam Oil Using Molecular Docking Analysis for Fatty Acid Specificity. *Biotechnol. Appl. Biochem.* **2019**, *66*, 823–832. [[CrossRef](#)]
45. Brandão, L.M.d.S.; Barbosa, M.S.; Souza, R.L.; Pereira, M.M.; Lima, Á.S.; Soares, C.M.F. Lipase Activation by Molecular Bioimprinting: The Role of Interactions between Fatty Acids and Enzyme Active Site. *Biotechnol. Prog.* **2021**, *37*, e3064. [[CrossRef](#)]
46. Rodrigues, C.A.; Barbosa, M.S.; Santos, J.C.B.; Lisboa, M.C.; Souza, R.L.; Pereira, M.M.; Lima, Á.S.; Soares, C.M.F. Computational and Experimental Analysis on the Preferential Selectivity of Lipases for Triglycerides in Licuri Oil. *Bioprocess Biosyst. Eng.* **2021**, *44*, 2141–2151. [[CrossRef](#)]
47. Gao, W.W.; Zhang, F.X.; Zhang, G.X.; Zhou, C.H. Key Factors Affecting the Activity and Stability of Enzymes in Ionic Liquids and Novel Applications in Biocatalysis. *Biochem. Eng. J.* **2015**, *99*, 67–84. [[CrossRef](#)]
48. Zheng, M.; Xiang, X.; Wang, S.; Shi, J.; Deng, Q.; Huang, F.; Cong, R. Lipase Immobilized in Ordered Mesoporous Silica: A Powerful Biocatalyst for Ultrafast Kinetic Resolution of Racemic Secondary Alcohols. *Process Biochem.* **2017**, *53*, 102–108. [[CrossRef](#)]
49. Rodrigues, M.I.; Iemma, A.F. *Experimental Design and Process Optimization*; CRC Press: Boca Raton, FL, USA, 2014. [[CrossRef](#)]
50. Trott, O.; Olson, A.J. AutoDock Vina: Improving the Speed and Accuracy of Docking with a New Scoring Function, Efficient Optimization, and Multithreading. *J. Comput. Chem.* **2010**, *31*, 455–461. [[CrossRef](#)] [[PubMed](#)]
51. Morris, G.M.; Huey, R.; Lindstrom, W.; Sanner, M.F.; Belew, R.K.; Goodsell, D.S.; Olson, A.J. AutoDock4 and AutoDockTools4: Automated Docking with Selective Receptor Flexibility. *J. Comput. Chem.* **2009**, *30*, 2785–2791. [[CrossRef](#)] [[PubMed](#)]

Disclaimer/Publisher’s Note: The statements, opinions and data contained in all publications are solely those of the individual author(s) and contributor(s) and not of MDPI and/or the editor(s). MDPI and/or the editor(s) disclaim responsibility for any injury to people or property resulting from any ideas, methods, instructions or products referred to in the content.